Searching for an exotic spin-dependent interaction between electrons at the nanometer scale with molecular rulers

Man Jiao,[1,2,3] Xing Rong,[1,2,3,*] Hang Liang,[1,2,3] Yi-Fu Cai,[4,5] and Jiangfeng Du[1,2,3,†]

[1]*Hefei National Laboratory for Physical Sciences at the Microscale and Department of Modern Physics, University of Science and Technology of China, Hefei 230026, China*

[2]*CAS Key Laboratory of Microscale Magnetic Resonance, University of Science and Technology of China, Hefei 230026, China*

[3]*Synergetic Innovation Center of Quantum Information and Quantum Physics, University of Science and Technology of China, Hefei 230026, China*

[4]*CAS Key Laboratory for Research in Galaxies and Cosmology, Department of Astronomy, University of Science and Technology of China, Hefei 230026, China*

[5]*School of Astronomy and Space Science, University of Science and Technology of China, Hefei 230026, China*

(Received 7 April 2019; revised manuscript received 25 April 2020; accepted 27 May 2020; published 11 June 2020)

We propose a new scheme to constrain an exotic spin-dependent interaction between electrons at the nanometer scale. Molecular rulers containing two electron spins and a shape-persistent polymer chain are utilized in the scheme. The distances between electron spins can be tuned by varying the lengths of the polymer chains connecting the two electron spins. With the measurement of the coupling strength between electron spins, improved laboratory bounds of axial-vector mediated interaction are established in the force range from 3 to 200 nm. The upper limit of the coupling $g_A^e g_A^e/4\pi\hbar c$ for the force range of 200 nm is $|g_A^e g_A^e/4\pi\hbar c| \leq 1.0 \times 10^{-12}$, which improves the previous limit on $g_A^e g_A^e/4\pi\hbar c$ by 1 order of magnitude.

DOI: 10.1103/PhysRevD.101.115011

Light bosons such as pseudoscalar fields (axion and axionlike particles [1,2]) and axial-vector fields (paraphotons and extra Z bosons) are hypothetically expected to address mysteries of fundamental sciences, namely, the microscopic origins of dark matter and dark energy, the resolution to the strong *CP* issue in quantum chromodynamics, as well as the possible connection with the hierarchy problem [3]. The exchange of such bosons may mediate exotic spin-dependent interactions between ordinary fermions, which enables us to search for the bosons through the laboratory method [2,4–6]. The exotic spin-dependent interactions between fermions are characterized by dimensionless coupling constants and decay rapidly with distance between fermions [4,5]. Since the force ranges of the exotic interactions, which are associated with the masses of mediating bosons are unknown, it is important to utilize various experiments working at force ranges from the atomic scale to the radius of the Earth [6]. For the force range below micrometer scale, stringent upper limits of the exotic interactions are provided by exquisite experiments, such as nitrogen-vacancy centers in diamond [7], trapped ions [8], single-atom electron spin resonance with scanning tunneling microscope (ESR-STM) [9–11], and atomic spectroscopy [12,13]. The upper limits of the exotic interactions are limited by the sensitivities of experimental measurements.

In this paper, we propose a novel method to search for axial-vector-mediated exotic spin-dependent interaction between electrons at the nanometer scale. The molecular rulers, which consist of two electron spins and a shape-persistent polymer chain, are used to search for the exotic spin-dependent interaction. Polymer chains composed of p-phenylene (PP) and ethynylene (E) are widely used in the construction of nanostructures due to their good synthetic accessibility and unambiguous geometrical structure [14]. Here, rodlike moieties consisting of PP and E are the spacers connecting the two electron spins. The distance between two electron spins can be tuned by synthesizing molecular rulers with different sequences of PP and E units. In addition, the shape-persistent spacers contribute to narrow distance distributions between two electron spins. Coupling strength between two electron spins is obtained by double electron-electron resonance (DEER) experiments. Based on these measurements, we establish new experimental constraints on the exotic interaction between electrons, which considerably improve previous bounds at the nanometer scale.

Figure 1(a) demonstrates a schematic diagram of two electron spins in an external magnetic field. The magnetic dipole-dipole interaction between two electron spins is described by the following Hamiltonian:

*xrong@ustc.edu.cn
†djf@ustc.edu.cn

$$V_d = -\frac{\mu_0 g_1 g_2 \mu_B^2}{4\pi r^3}[3(\vec{S}_1 \cdot \hat{r})(\vec{S}_2 \cdot \hat{r}) - (\vec{S}_1 \cdot \vec{S}_2)], \quad (1)$$

where $\vec{S}_1$ and $\vec{S}_2$ stand for spin operators of the two electron spins, $\vec{S}_i = \vec{\sigma}_i/2$, $i = 1, 2$. $\vec{\sigma}_1$ and $\vec{\sigma}_2$ are Pauli vectors of the two electron spins. μ_0 is the vacuum permeability. g_1 and g_2 are g factors of the two electron spins. μ_B is the Bohr magneton constant. $r = |\vec{r}|$ is the displacement between two electron spins, and $\hat{r} = \vec{r}/r$ is unit displacement vector between two electron spins. The exchange of a hypothetical axial-vector boson leads to exotic dipole-dipole interaction: [4]

$$V_2 = \frac{g_A^e g_A^e}{4\pi\hbar c}\frac{\hbar c}{r} e^{-\frac{r}{\lambda}}(\vec{\sigma}_1 \cdot \vec{\sigma}_2), \quad (2)$$

where $g_A^e g_A^e/4\pi\hbar c$ is the dimensionless coupling constant. $\lambda = \hbar/(mc)$ is the reduced Compton wavelength of the hypothetical axial-vector boson of mass m. c is the speed of light.

Molecular rulers used in this work consist of different sequences of PP, E, and two Gd-PyMTA spin labels. Gd-PyMTA has a Gd^{3+} ion center and the electron spin of Gd^{3+} is in the ^8S ground state. With seven unpaired electrons in its f orbital, the Gd^{3+} spin label has an effective electron spin of $S = 7/2$. The zero-field splitting of the Gd-PyMTA spin label is 1150 MHz [15]. The g factors of Gd^{3+} spin labels are 1.9925, which are obtained from the molecules with only one Gd^{3+} spin label [16]. The g factors obtained from Ref. [16] are not influenced by the exotic spin-dependent interaction, since the exotic interaction does not exist in molecules with only one Gd^{3+} spin label. Meanwhile, in the high magnetic field Electron Paramagnetic Resonance (EPR) experiments, the variation in g factors between Gd^{3+} complexes with different ligands is negligible [16]. The rodlike moieties made up of PP and E keep two Gd^{3+} spin labels at a well-defined distance. Ball-and-stick models of the molecules are shown in Fig. 1(b). The molecules are denoted as Gd-rulers $\mathbf{1_n}$ ($n = 5, 7, 9, 11$) and $\mathbf{2_2}$. Notations 1 and 2 represent two types of molecular structures, and the subscripts denote the number of repeating units. The synthesis of the geometrically well-defined Gd-rulers are reported in Ref. [17].

The coupling strength between two electron spins in the Gd-rulers are measured by DEER experiments [15]. The DEER experiment is a powerful tool to measure dipolar coupling strength between spin labels, which are separated in the nanometer scale. In the W-band DEER experiments in Ref. [15], two Gd^{3+} spin labels in Gd-rulers can be considered as a pair of weakly coupled spins with $S = 1/2$ (see Appendix A). The magnetic dipole-dipole interaction and the exotic interaction between two Gd^{3+} spin labels can be estimated by the secular terms of the interaction Hamiltonian:

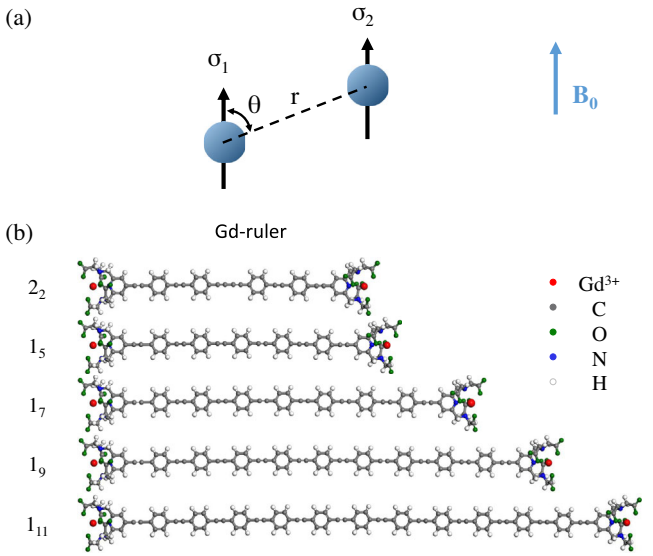

FIG. 1. (a) A schematic diagram of two coupled electron spins (σ_1 and σ_2) in an external magnetic field B_0. $\mathbf{r}$ is the displacement vector between two electron spins. θ stands for the angle between the displacement vector and the external magnetic field $\mathbf{B_0}$. (b) Ball-and-stick models of molecular rulers. $\mathbf{1_n}$ ($n = 5, 7, 9, 11$) and $\mathbf{2_2}$ are the notations associated with the five molecular rulers, respectively. The notations 1 and 2 represent two types of molecular structures. The subscripts denote the number of repeating units. For Gd-rulers $\mathbf{2_n}$, n repeating units appear twice in the molecules, so the Gd-ruler $\mathbf{2_2}$ has four repeating units with benzene. The red dots, dark gray dots, green dots, blue dots, and the light gray circles denote gadolinium atoms, carbon atoms, oxygen atoms, nitrogen atoms, and hydrogen atoms, respectively.

$$\begin{cases} V_d^{\text{secular}} = -\frac{\mu_0 g_1 g_2 \mu_B^2}{4\pi r^3}(3\cos^2\theta - 1)S_1^z S_2^z, \\ V_2^{\text{secular}} = \frac{g_A^e g_A^e}{4\pi\hbar c}\frac{\hbar c}{r} e^{-\frac{r}{\lambda}}\sigma_1^z \sigma_2^z. \end{cases} \quad (3)$$

Details of the DEER experiments [15] are provided in Appendix B. Briefly, the DEER experiments were carried out at 10 K using a home-built W-band (94.9 GHz) spectrometer [15]. The samples were diluted in a 7:3 (volume ratio) mixture of D_2O and glycerol-d_8, the concentrations of Gd-rulers $\mathbf{1_5}$, $\mathbf{1_7}$, $\mathbf{1_9}$, $\mathbf{1_{11}}$, and $\mathbf{2_2}$ are 0.1, 0.1, 0.05, 0.1, and 0.03 mM, respectively. A four-pulse sequence was applied to Gd-rulers in the DEER experiments. The detected echo intensity is modulated by the dipolar coupling strength (see Appendix A).

Figure 2 shows the experimental results adopted from Ref. [15]. We take the magnetic dipole-dipole interactions into account at first. Other interactions, such as exchange interactions between electron spins and intramolecule interactions, are negligible [15]. Because of the random orientations of the molecular axes in the frozen solution and the flexibility of Gd-rulers, echo intensities decay with time as discussed in Appendix A. By fitting the echo intensity function to experimental DEER traces, the distance between Gd^{3+} electron spins and the FWHM of distance

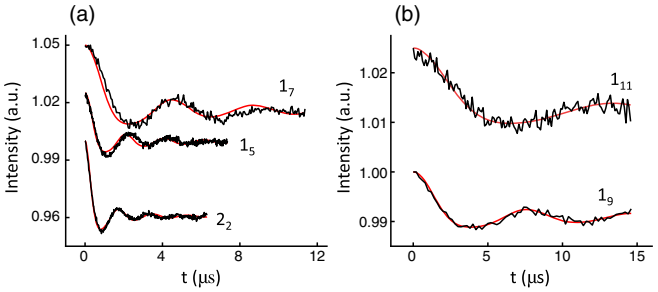

FIG. 2. DEER measurements adopted from Ref. [15] (black lines) and fitting results (red lines). (a) Experimental results of molecular ruler $\mathbf{1_5}$, $\mathbf{1_7}$, and $\mathbf{2_2}$. (b) Experimental results of molecular ruler $\mathbf{1_9}$ and $\mathbf{1_{11}}$. Red lines are fittings with the echo intensity function as discussed in Appendix A. Intensity offsets are added manually.

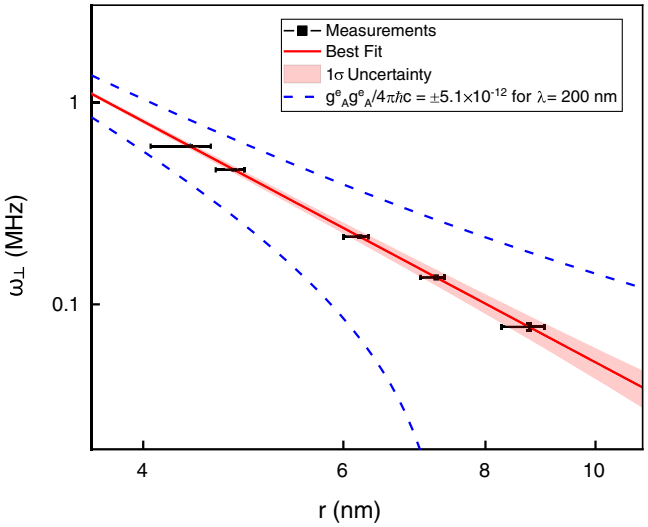

FIG. 3. Coupling strength $\omega_\perp$ as a function of distance, r. Data points and the error bars are derived from the fitting of time domain DEER traces. The red solid line is the best fit with Eq. (4) when $\lambda = 200$ nm gives $g_A^e g_A^e/4\pi\hbar c = (0.0 \pm 5.1) \times 10^{-13}$. The shaded region is a 1σ uncertainty band of the fit. Blue dashed lines show the hypothetical signals when $g_A^e g_A^e/4\pi\hbar c = \pm 5.1 \times 10^{-12}$ with $\lambda = 200$ nm, and the linearity of the exotic interaction V_2 is similar to the exponential in logarithmic coordinate.

distributions are obtained. More details of the fitting are discussed in Appendix B. The Gd-Gd distance and HWHM for Gd-rulers $\mathbf{2_2}$, $\mathbf{1_5}$, $\mathbf{1_7}$, $\mathbf{1_9}$, and $\mathbf{1_{11}}$ are 4.4(0.5), 4.8(0.3), 6.2(0.3), 7.2(0.4), and 8.7(0.8) nm. The experimental coupling strength with $\theta = \pi/2$ for different distances can be obtained. In addition, distances from fitting results are in good agreement with distances derived from density functional theory (DFT) calculations (see Fig. 6 in Appendix B).

Then we take the hypothetical exotic interaction into account. The coupling strength between two Gd^{3+} electron spins with $\theta = \pi/2$ is

$$\omega_\perp = \frac{\mu_0 g_1 g_1 \mu_B^2}{4\pi h}\frac{1}{r^3} + \frac{g_A^e g_A^e}{4\pi\hbar c}\frac{4\hbar c}{h}\frac{e^{-\frac{r}{\lambda}}}{r}. \quad (4)$$

In the assumption of the coupling strength, where the measurement in the DEER experiments is contributed from both the magnetic dipole-dipole interaction and the axial-vector exotic interaction, fittings with $\omega_\perp$ were made to derive the coupling constants $g_A^e g_A^e/4\pi\hbar c$ of the exotic axial-vector-mediated interaction. The experimental results and a fitting at $\lambda = 200$ nm are presented in Fig. 3. The x values of data points are the distances with max probability in the distance distribution of the Gd-rulers. Error bars in the x dimension denote distance distributions due to the flexibility. The distance distributions of Gd-rulers are asymmetric about the center, which is discussed in Appendix B. Error bars on the coupling strength are calculated by the fitting errors of distances according to the error transfer formula.

The red line in Fig. 3 is the best fit with Eq. (4) when the force range $\lambda = 200$ nm. The coupling constant of the exotic axial-vector-mediated interaction for $\lambda = 200$ nm is obtained to be $g_A^e g_A^e/4\pi\hbar c = (0.0 \pm 5.1) \times 10^{-13}$. The value of the axial-vector field induced interaction is less than its errors showing no evidence of the exotic interaction observed in these measurements. The upper limit of the exotic interaction at $\lambda = 200$ nm is $g_A^e g_A^e/4\pi\hbar c \leq 1.0 \times 10^{-12}$ with 95% confidence level. The shaded region is the 1σ uncertainty band of the fit. Blue dashed lines show the hypothetical signals when $g_A^e g_A^e/4\pi\hbar c = \pm 5.1 \times 10^{-12}$ with $\lambda = 200$ nm. In the log-log plot, the power law magnetic dipole-dipole interaction is a straight line, while the linearity of the exotic interaction V_2 is similar to the exponential. The hypothetical signals are obviously different from the experimental results. To obtain the constraints for other force ranges, we repeat the fitting for different force ranges, and then obtain the upper limits of $g_A^e g_A^e/4\pi\hbar c$ with the 95% confidence level according to the fitting results.

Figure 4 shows the experimental constraints on the axial-vector exotic interaction V_2 by this work and previous results from Refs. [7,8,11,13,18]. The bottom axis corresponds to the force range of the interaction, which is inversely proportional to the mass of the mediating boson in the top axis. The vertical axis represents the dimensionless coupling constant $g_A^e g_A^e/4\pi\hbar c$ between electrons. Filled areas indicate excluded regions. For the force range $\lambda < 3$ nm, the upper limits were obtained from Ref. [13]. The red line in Fig. 4 shows the constraints established in this work, which are more stringent than previous bounds in the range from 3 to 200 nm. For the force range from 10 to 200 nm, previous limits were set by Luo *et al.* [11] with precise ESR-STM experiments [9]. For the force range $0.22\ \mu\text{m} < \lambda < 10\ \mu\text{m}$, the constraints were established by Kotler *et al.* [8]. Upper limits in the range from 10 to 900 μm were set by Rong *et al.* [7]. Ritter *et al.* [18] set constraints in the force range in the millimeter scale and

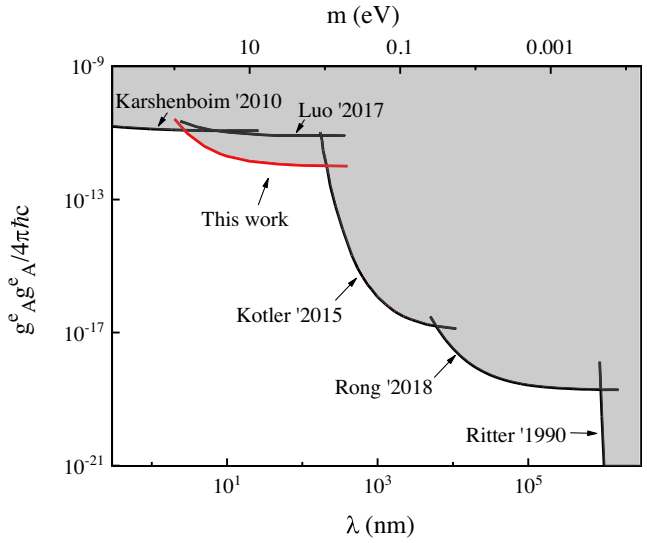

FIG. 4. The experimental constraints on the axial-vector-mediated dipole-dipole interactions between electrons as a function of the force range λ and the mass of the axial-vector boson m. Solid black lines represent upper bounds obtained from Refs. [7,8,11,13,18]. This work establishes new laboratory bounds in the force range from 3 to 200 nm (the red line). The obtained upper limit at $\lambda = 200$ nm is $|g^e_A g^e_A/4\pi\hbar c| \leq 1.0 \times 10^{-12}$, which improves the previous limit on $g^e_A g^e_A/4\pi\hbar c$ by 1 order of magnitude.

above. Specifically, the obtained upper limit from our method improves the previous limit by 1 order of magnitude at $\lambda = 200$ nm. Benefiting from the pulse EPR technique, our method provides a better precision of detection for coupling strength between two electrons compared to the ESR-STM experiments.

In summary, we provide a novel method to search for an exotic spin-dependent interaction at the nanometer scale. Improved constraints on the axial-vector-mediated interaction between electrons are established. Furthermore, DEER measurements have been carried out on molecules with triple electron spins of Gd^{3+}, Mn^{2+}, and a nitroxide [19]. Measurements based on chemically synthesized molecules may provide new possibilities for searching for exotic spin-dependent interactions. We also expect that electron spins of molecular rulers with longer coherence times can be synthesized for this study. With longer coherence times, a better precision can be achieved, and the constraints can be further improved.

We noticed that a revisiting of spin-dependent interactions has recently been proposed [5]. We expect experiments with molecular rulers can be utilized to provide constraints on the interactions in the future.

The authors thank Professor Dieter Suter for helpful discussion. We are also grateful to Professor Daniella Goldfarb for sharing the experimental data of the DEER experiments with us. We do appreciate Xiaojing Liu for the DFT calculations. This work was supported by the National Key R&D Program of China (Grants No. 2018YFA0306600 and No. 2016YFB0501603), the Chinese Academy of Sciences (Grants No. GJJSTD20170001, No. QYZDY-SSW-SLH004, and No. QYZDB-SSW-SLH005), and the Anhui Initiative in Quantum Information Technologies (Grant No. AHY050000). X. R. thanks the Youth Innovation Promotion Association of the Chinese Academy of Sciences for support. Y. F. C is supported in part by the NSFC (Grants No. 11653002 and No. 11722327), by the National Youth Thousand Talents Program of China, by the CAST Young Elite Scientists Sponsorship Program (2016QNRC001), and by the Fundamental Research Funds for the Central Universities.

APPENDIX A: THE COUPLING BETWEEN Gd^{3+} ELECTRON SPINS

Equation (3) in the main text is the secular term of the interaction Hamiltonian between two Gd^{3+} electron spins. Because of the high magnetic field and the zero-field splitting, only secular terms of dipolar interaction remain for two Gd^{3+} electron spins [15,20]. The DEER experiments in Ref. [15] chose the central transition frequency of the EPR spectrum and 90 MHz (3.2 mT) higher as the resonance frequency for observe and pump spins. Four energy subspaces $|-3/2_{\text{observe}}\rangle$, $|-1/2_{\text{observe}}\rangle$, $|-1/2_{\text{pump}}\rangle$, and $|1/2_{\text{pump}}\rangle$ made the major contribution to the DEER spectrum. Thus, the Gd^{3+} spin pair can be considered as a weakly coupled spin pair with $S = 1/2$. Moreover, Ref. [15] compared DEER results of Gd^{3+} and nitroxyl spin labels. The values of distances derived from Gd-rulers are in good agreement with the distance derived from nitroxyl rulers, which suggests Gd-Gd can be treated as a spin-half pair. In conclusion, the Gd^{3+} electron spin pair can be treated as a pair of weakly coupled spins with $S = 1/2$. The interaction can be estimated by Eq. (3), using the sigma matrix denoting Gd^{3+} electron spins.

APPENDIX B: TIME DOMAIN DEER TRACE AND DETAIL OF THE FITTING

DEER experiments were performed at 10 K using a home-built W-band (94.9 GHz) spectrometer with a magnetic field of about 3400 mT. A four-pulse sequence with two pulse frequencies corresponding to the observe and pump spin resonance frequencies was applied. Reference [21] provides a detailed description and characterization of the four-pulse sequence. The detected echo intensity denotes magnetization in the x-y plane in the Bloch sphere of the observe spin. Because of the dipolar interaction between two Gd^{3+} electron spins, the observe spin acquires a phase shift in the x-y plane of the Bloch sphere. Through varying the timing of the π pulse applied on the pump spin, the echo intensity of the observe spin is modulated by the coupling strength, as shown in Fig. 2 in the main text.

The echo intensity of the time domain DEER trace can be interpreted as [22]

$$V(t) = V_0\left\{1 - \lambda_{md} \times \left[1 + \int_0^{\infty}\int_0^{\pi/2} \cos(\omega_{dd}(\theta, r)t)P(r)P(\theta)d\theta dr\right]\right\}, \tag{B1}$$

$$\omega_{dd} = \frac{\mu_0 g_1 g_1 \mu_B^2}{4\pi h}\frac{3\cos^2\theta - 1}{r^3}, \tag{B2}$$

where V_0 is the echo intensity of the twice refocused Hahn-echo sequence of the observe spin. λ_{md} is the modulation depth, representing the fraction of spins excited by the pump pulse. $P(r)$ is the Gd-Gd distance distribution of Gd-rulers. θ is the angle of the molecule with respect to the magnetic field B_0. Echo intensity is an integration of θ with a weighting of $P(\theta) = \sin(\theta)$. The distance distribution of the rigid molecules can be estimated by the harmonic segmented chain model. The distance distribution is determined by the bending potential and the thermal energy [14]. Here we take Gd-ruler 1_{11} as an example. The distance distribution derived from HSC model is shown in Fig. 5 with the FWHM of the distance distribution being 0.397 nm.

By fitting the echo intensity function equations, (B1) and (B2), to experimental DEER traces, the distance between Gd^{3+} electron spins and the FWHM of the distance distribution are obtained. The distance between Gd^{3+} can also be estimated from DFT. We used scalar relativistic DFT as implemented in the Gaussian software package [23] and performed full geometry optimizations for all structures. In our DFT calculations, the three-parameter hybrid exchange functional of Becke and the exchange functional of Lee-Yang-Parr (B3LYP) [24–26] was employed. More precisely, to ensure a correct approach for the open-shell species, we employed the spin-unrestricted open-shell version of this functional (UB3LYP). The standard basis set 6-31G(d) is used for C, H, and N atoms while the Stuttgart RSC 1997 ECP basis set [27] is used for Gd atom. The DFT results show that Gd-Gd distance for Gd-rulers $\mathbf{2_2}$, $\mathbf{1_5}$, $\mathbf{1_7}$, $\mathbf{1_9}$, and $\mathbf{1_{11}}$, are 4.25, 4.70, 6.05, 7.41, and 8.78 nm, respectively, which are in good agreement with the distances derived from the fitting of time domain DEER traces.

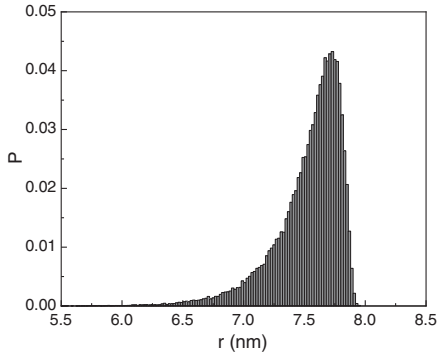

FIG. 5. Histogram of distance distributions of 10^5 calculations for the Gd-ruler 1_{11} backbone.

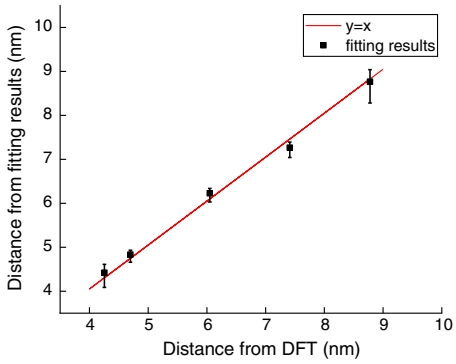

FIG. 6. Gd-Gd distance obtained by fitting results versus Gd-Gd distance calculated by DFT. The solid line indicates where the data points should be if the Gd-Gd distance determined by fitting and DFT calculations are identical.

[1] S. Weinberg, A New Light Boson?, Phys. Rev. Lett. **40**, 223 (1978).
[2] J. Moody and F. Wilczek, New macroscopic forces?, Phys. Rev. D **30**, 130 (1984).
[3] J. L. Feng, Dark matter candidates from particle physics and methods of detection, Annu. Rev. Astron. Astrophys. **48**, 495 (2010).
[4] B. A. Dobrescu and I. Mocioiu, Spin-dependent macroscopic forces from new particle exchange, J. High Energy Phys. 11 (2006) 005.
[5] P. Fadeev, Y. V. Stadnik, F. Ficek, M. G. Kozlov, V. V. Flambaum, and D. Budker, Revisiting spin-dependent forces mediated by new bosons: Potentials in the coordinate-space representation for macroscopic- and atomic-scale experiments. Phys. Rev. A **99**, 022113 (2019).
[6] M. S. Safronova, D. Budker, D. DeMille, D. F. Jackson Kimball, A. Derevianko, and C. W. Clark, Search for new physics with atoms and molecules, Rev. Mod. Phys. **90**, 025008 (2018).
[7] X. Rong, M. Jiao, J. Geng, B. Zhang, T. Xie, F. Shi, C.-K. Duan, Y.-F. Cai, and J. Du, Constraints on a Spin-Dependent Exotic Interaction between Electrons with Single Electron Spin Quantum Sensors, Phys. Rev. Lett. **121**, 080402 (2018).

[8] S. Kotler, R. Ozeri, and D. F. J. Kimball, Constraints on Exotic Dipole-Dipole Couplings between Electrons at the Micrometer Scale, Phys. Rev. Lett. **115**, 081801 (2015).
[9] T. Choi, W. Paul, S. Rolf-Pissarczyk, A. J. Macdonald, F. D. Natterer, K. Yang, P. Willke, C. P. Lutz, and A. J. Heinrich, Atomic-scale sensing of the magnetic dipolar field from single atoms, Nat. Nanotechnol. **12**, 420 (2017).
[10] S. Baumann, W. Paul, T. Choi, C. P. Lutz, A. Ardavan, and A. J. Heinrich, Electron paramagnetic resonance of individual atoms on a surface, Science **350**, 417 (2015).
[11] P. Luo, J. Ding, J. Wang, and X. Ren, Constraints on spin-dependent exotic interactions between electrons at the nanometer scale, Phys. Rev. D **96**, 055028 (2017).
[12] F. Ficek, D. F. Jackson Kimball, M. G. Kozlov, N. Leefer, S. Pustelny, and D. Budker, Constraints on exotic spin-dependent interactions between electrons from helium fine-structure spectroscopy, Phys. Rev. A **95**, 032505 (2017).
[13] S. G. Karshenboim, Precision Physics of Simple Atoms and Constraints on a Light Boson with Ultraweak Coupling, Phys. Rev. Lett. **104**, 220406 (2010).
[14] G. Jeschke, M. Sajid, M. Schulte, N. Ramezanian, A. Volkov, H. Zimmermann, and A. Godt, Flexibility of shape-persistent molecular building blocks composed of p-phenylene and ethynylene units, J. Am. Chem. Soc. **132**, 10107 (2010).
[15] A. Dalaloyan, M. Qi, S. Ruthstein, S. Vega, A. Godt, A. Feintuch, and D. Goldfarb, Gd (III)–Gd (III) EPR distance measurements–the range of accessible distances and the impact of zero field splitting, Phys. Chem. Chem. Phys. **17**, 18464 (2015).
[16] S. Rast, A. Borel, L. Helm, E. Belorizky, P. H. Fries, and A. E. Merbach, EPR spectroscopy of MRI-Related Gd(III) complexes: Simultaneous analysis of multiple frequency and temperature spectra, including static and transient crystal field effects, J. Am. Chem. Soc. **123**, 2637 (2001).
[17] M. Qi, M. Hülsmann, and A. Godt, Spacers for geometrically well-defined water-soluble molecular rulers and their application, J. Org. Chem. **81**, 2549 (2016).
[18] R. C. Ritter, Experimental test of equivalence principle with polarized masses, Phys. Rev. D **42**, 977 (1990).
[19] Z. Wu, A. Feintuch, A. Collauto, L. A. Adams, L. Aurelio, B. Graham, G. Otting, and D. Goldfarb, Selective distance measurements using triple spin labeling with Gd^{3+}, Mn^{2+}, and a nitroxide, J. Phys. Chem. Lett. **8**, 5277 (2017).
[20] D. Goldfarb, Gd^{3+} spin labeling for distance measurements by pulse EPR spectroscopy, Phys. Chem. Chem. Phys. **16**, 9685 (2014).
[21] M. Pannier, S. Veit, A. Godt, G. Jeschke, and H. W. Spiess, Dead-time free measurement of dipole–dipole interactions between electron spins. J. Magn. Reson., **142**, 331 (2000).
[22] N. Manukovsky, A. Feintuch, I. Kuprov, and D. Goldfarb, Time domain simulation of Gd^{3+}–Gd^{3+} distance measurements by EPR, J. Chem. Phys. **147**, 044201 (2017).
[23] M. J. Frisch *et al.*, *Gaussian 16 Revision B.01* (Gaussian Inc., Wallingford, CT, 2016).
[24] C. Lee, W. Yang, and R. G. Parr, Development of the colle-salvetti correlation-energy formula into a functional of the electron density, Phys. Rev. B **37**, 785 (1988).
[25] A. D. Becke, Density-functional thermochemistry. III. The role of exact exchange, J. Chem. Phys. **98**, 5648 (1993).
[26] A. D. Becke, Density-functional exchange-energy approximation with correct asymptotic behavior, Phys. Rev. A **38**, 3098 (1988).
[27] D. Andrae, U. Häußermann, M. Dolg, H. Stoll, and H. Preuß, Energy-adjusted *ab initio* pseudopotentials for the second and third row transition elements, Theor. Chim. Acta **77**, 123 (1990).